True-time delay line with separate carrier tuning using dual-parallel MZM and stimulated Brillouin scattering-induced slow light

Wei Li,* Ning Hua Zhu, Li Xian Wang, Jia Sheng Wang, Jian Guo Liu, Yu Liu, Xiao Qiong Qi, Liang Xie, Wei Chen, Xin Wang, and Wei Han

State Key Laboratory on Integrated Optoelectronics, Institute of Semiconductors, Chinese Academy of Sciences, Beijing, 100083, China
**liwei05@semi.ac.cn*

Abstract: We experimentally demonstrate a novel tunable true-time delay line with separate carrier tuning using dual-parallel Mach-Zehnder modulator and stimulated Brillouin scattering-induced slow light. The phase of the optical carrier can be continuously and precisely controlled by simply adjusting the dc bias of the dual-parallel Mach-Zehnder modulator. In addition, both the slow light and single-sideband modulation can be simultaneously achieved in the stimulated Brillouin scattering process with three types of configuration. Finally, the true-time delay technique is clearly verified by a two-tap incoherent microwave photonic filter as the free spectral range of the filter is changed.

OCIS codes: (060.4370) Non-linear optics, fibers; (290.5900) Scattering, stimulated Brillouin; (070.1170) Analogue signal processing; (999.9999) Slow light.

References and links

1. J. Yao, "Microwave photonics," J. Lightwave Technol. **27**(3), 314–335 (2009).
2. J. Capmany, and D. Novak, "Microwave photonics combines two worlds," Nat. Photonics **1**(6), 319–330 (2007).
3. R. J. Mailloux, *Phased Array Antenna Handbook* (Artech, 1994).
4. W. Ng, A. A. Walston, G. L. Tangonan, J. J. Lee, I. L. Newberg, and N. Bernstein, "The first demonstration of an optically steered microwave phased array antenna using true-time-delay," J. Lightwave Technol. **9**(9), 1124–1131 (1991).
5. R. D. Esman, M. Y. Frankel, J. L. Dexter, L. Goldberg, M. G. Parent, D. Stilwell, and D. G. Cooper, "Fiber-optic prism true time-delay antenna feed," IEEE Photon. Technol. Lett. **5**(11), 1347–1349 (1993).
6. J. L. Corral, J. Marti, J. M. Fuster, and R. I. Laming, "True time-delay scheme for feeding optically controlled phased-array antennas using chirped-fiber gratings," IEEE Photon. Technol. Lett. **9**(11), 1529–1531 (1997).
7. J. Mørk, R. Kjær, M. van der Poel, and K. Yvind, "Slow light in a semiconductor waveguide at gigahertz frequencies," Opt. Express **13**(20), 8136–8145 (2005).
8. Y. Okawachi, M. S. Bigelow, J. E. Sharping, Z. Zhu, A. Schweinsberg, D. J. Gauthier, R. W. Boyd, and A. L. Gaeta, "Tunable all-optical delays via Brillouin slow light in an optical fiber," Phys. Rev. Lett. **94**(15), 153902 (2005).
9. H. Su, P. Kondratko, and S. L. Chuang, "Variable optical delay using population oscillation and four-wave-mixing in semiconductor optical amplifiers," Opt. Express **14**(11), 4800–4807 (2006).
10. M. V. Drummond, P. P. Monteiro, and R. N. Nogueira, "Photonic true-time delay beamforming based on polarization-domain interferometers," J. Lightwave Technol. **28**(17), 2492–2498 (2010).
11. S. Sales, W. Xue, J. Mørk, and I. Gasulla, "Slow and fast light effects and their applications to microwave photonics using semiconductor optical amplifiers," IEEE Trans. Microw. Theory Tech. **58**(11), 3022–3038 (2010).
12. M. D. Stenner, M. A. Neifeld, Z. Zhu, A. M. C. Dawes, and D. J. Gauthier, "Distortion management in slow-light pulse delay," Opt. Express **13**(25), 9995–10002 (2005).
13. M. González Herráez, K. Y. Song, and L. Thévenaz, "Arbitrary-bandwidth Brillouin slow light in optical fibers," Opt. Express **14**(4), 1395–1400 (2006).
14. Z. Zhu, A. M. C. Dawes, D. J. Gauthier, L. Zhang, and A. E. Willner, "Broadband SBS slow light in an optical fiber," J. Lightwave Technol. **25**(1), 201–206 (2007).
15. E. Cabrera-Granado, O. G. Calderón, S. Melle, D. J. Gauthier; E. C. Granado, "Observation of large 10-Gb/s SBS slow light delay with low distortion using an optimized gain profile," Opt. Express **16**(20), 16032–16042 (2008).
16. T. Schneider, "Time delay limits of stimulated-Brillouin-scattering-based slow light systems," Opt. Lett. **33**(13), 1398–1400 (2008).

#145830 - $15.00 USD Received 14 Apr 2011; revised 1 Jun 2011; accepted 2 Jun 2011; published 9 Jun 2011

17. P. A. Morton, and J. B. Khurgin, "Microwave photonic delay line with separate tuning of the optical carrier," IEEE Photon. Technol. Lett. **21**(22), 1686–1688 (2009).
18. J. Sancho, S. Chin, M. Sagues, A. Loayssa, J. Lloret, I. Gasulla, S. Sales, L. Thévenaz, and J. Capmany, "Dynamic microwave photonic filter using separate carrier tuning based on stimulated Brillouin scattering in fibers," IEEE Photon. Technol. Lett. **22**(23), 1753–1755 (2010).
19. S. Chin, L. Thévenaz, J. Sancho, S. Sales, J. Capmany, P. Berger, J. Bourderionnet, and D. Dolfi, "Broadband true time delay for microwave signal processing, using slow light based on stimulated Brillouin scattering in optical fibers," Opt. Express **18**(21), 22599–22613 (2010).
20. A. Loayssa, and F. J. Lahoz, "Broad-band RF photonic phase shifter based on stimulated Brillouin scattering and single-sideband modulation," IEEE Photon. Technol. Lett. **18**(1), 208–210 (2006).
21. G. H. Smith, D. Novak, and Z. Ahmed, "Overcoming chromatic-dispersion effects in fiber-wireless systems incorporating external modulators," IEEE Trans. Microw. Theory Tech. **45**(8), 1410–1415 (1997).
22. S. Li, X. Zheng, H. Zhang, and B. Zhou, "Compensation of dispersion-induced power fading for highly linear radio-over-fiber link using carrier phase-shifted double sideband modulation," Opt. Lett. **36**(4), 546–548 (2011).
23. M. Sagues, and A. Loayssa, "Swept optical single sideband modulation for spectral measurement applications using stimulated Brillouin scattering," Opt. Express **18**(16), 17555–17568 (2010).
24. Z. Zhu, A. M. C. Dawes, D. J. Gauthier, L. Zhang, and A. E. Willner, "12-GHz-Bandwidth SBS Slow Light in Optical Fibers," in proceedings of OFC 2006, paper PD1 (2006).

1. Introduction

Tunable photonic delay lines have attracted considerable attention due to their wide range of potential applications [1,2], such as phased array antennas (PAA), microwave photonic filters (MPF) and arbitrary waveform generators. In PAA, true-time delay (TTD) beamforming is an effective way to solve the well-known beam squint problem [3]. Similarly, TTDs have also to be introduced to most MPFs which rely on discrete-time signal processing using real valued coefficients.

Among various optical TTD techniques [4–11], stimulated Brillouin scattering- (SBS) induced slow light has been extensively investigated as one promising approach to provide all-optically controlled and continuously tunable signal delaying [8,12–16]. However, the slow light-induced TTDs suffer from the limitation that the product between the maximum delay time and the signal bandwidth is constant. As a result, only modest time delay can be expected for broadband baseband signals. On the other hand, for optical communication systems, the small bandwidth of the SBS gain profile (~40 MHz in standard optical fibers) results in large distortion of the delayed pulses for data rates beyond 40 Mb/s using a monochromatic pump light [15]. However, the bandwidth limitation in SBS-based slow light can be overcome by pump spectral broadening technique [12–15]. In most broadband applications, the RF carrier frequency is much higher than the data signal bandwidth. It means that no information is carried in the wide frequency range between the optical carrier (OC) and the single-sideband (SSB) microwave envelope. In this context, a new concept of separate carrier tuning (SCT) has been proposed by Morton *et al.* to overcome this limitation [17]. Instead of having a constant time delay across the entire spectral bandwidth of the optical signal, the time delay only needs to be constant at the modulation sideband, as long as the phase of the OC is adjusted. Such concept relaxes the bandwidth requirement of the tunable delay lines down to the spectral bandwidth of the data signal which is modulated onto the RF carrier. It is especially important when high-frequency RF carriers are employed.

Recently, the validity of the SCT approach has been experimentally verified by Sancho and Chin *et al* [18,19]. In [18], a reconfigurable MPF has been demonstrated using a fiber Bragg grating (FBG) for OC phase-shifting and a SBS process for slow light system. However, the OC phase-shifting is unstable since FBG is sensitive to the environmental temperature and fluctuation. Moreover, the FBG leads to RF power variation when the phase of the OC is tuned since the optical power of OC is changed simultaneously. In order to overcome this problem, both OC phase compensator and slow light system have been implemented by SBS in [19]. The optical power of the OC remains unaltered when its phase is tuned by the SBS-induced phase shift since the gain and loss for the OC is mutually canceled out [19,20]. However, the use of two SBS processes makes the system complex and the lower RF frequency of the systems is limited to several gigahertz both in [18] and [19] by the bandwidth of the FBG notch filter, which is employed to block one of the modulation

#145830 - $15.00 USD Received 14 Apr 2011; revised 1 Jun 2011; accepted 2 Jun 2011; published 9 Jun 2011

sidebands to realize SSB modulation. Although the SSB modulation can be achieved by connecting a dual-driver Mach-Zehnder modulator (MZM) to quadrature inputs [21], a perfect 90° hybrid RF splitter where the outputs differ in phase by 90° over a wide RF bandwidth is still a challenge. Various techniques to achieving SSB modulation without relying on a non-perfect hybrid RF splitter should be pursued.

This paper presents a novel tunable TTD line with SCT using dual-parallel (DP) MZM and SBS-induced slow light. Compared with the OC phase-shifting methods reported in [18,19] using additional FBG or SBS-induced phase-shifting process, the phase of the OC in our method can be continuously and precisely tuned up to 360° by simply adjusting the dc bias of the modulator without using any complementary elements. This would significantly reduce the complexity of the system and increase the stability of the TTD line. In addition, both the SBS-induced slow light and SSB modulation can be simultaneously achieved in the SBS process without using any optical filters. Three types of SBS-induced slow light and SSB modulation configuration are demonstrated. On the other hand, the RF signal in the proposed method is frequency-tunable. In principle, the proposed technique works for arbitrarily high RF, which is only limited by the bandwidth of the optical transmitter and receiver employed. Finally, we apply the TTD line for an incoherent two-tap MPF for a proof-of-concept demonstration of our method.

2. Separate carrier tuning concept

We consider a SSB modulated optical signal comprising an OC and a single sideband at frequency ν_C and $\nu_C + \nu_{RF}$, respectively. In most broadband applications, the RF signal has a finite bandwidth $\Delta\nu_{RF}$ of typically 10~30% of the RF frequency ν_{RF}. Conventionally, TTD operation requires a pure and distortion-free delay on input RF signals, independently of the RF frequency, i.e. a linear phase slope across the entire spectral range between OC and the data sideband as shown in Fig. 1(a). The RF group delays is given by

$$T_{RF} = \frac{\phi(\nu_C + \nu_{RF}) - \phi(\nu_C)}{2\pi\nu_{RF}} \tag{1}$$

In Fig. 1(b), the SBS-induced slow light imparts a constant group delay over the frequency range $\Delta\nu_{RF}$ centered at frequency of $\nu_C + \nu_{RF}$, the signal delay time is given by:

$$T_S = \frac{1}{2\pi}\frac{\partial\phi}{\partial\nu}\bigg|_{\nu_C+\nu_{RF}}. \tag{2}$$

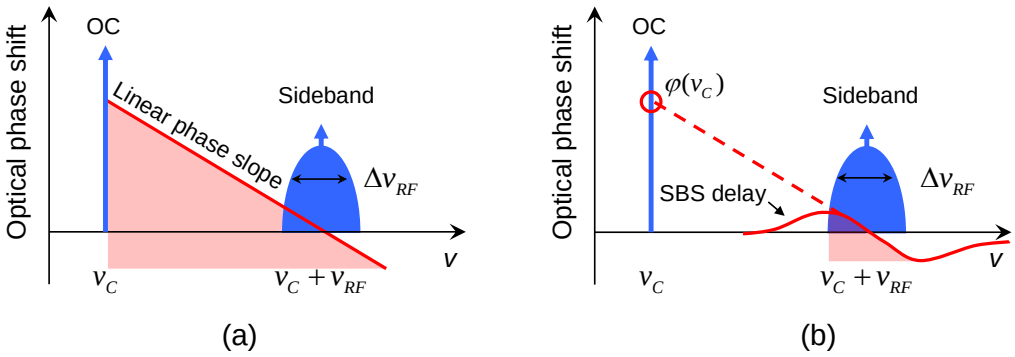

Fig. 1. Principle to perform TTD over the RF signal bandwidth $\Delta\nu_{RF}$ by (a) conventional method and (b) SCT technique.

Since no information is conveyed between the wide frequency range between OC and modulation sideband, according to the SCT concept, TTD operation over the entire RF frequency range can be simply achieved by imparting a proper phase shifting to OC to make signal and RF group delays match, deduced from the expression [19]:

#145830 - $15.00 USD Received 14 Apr 2011; revised 1 Jun 2011; accepted 2 Jun 2011; published 9 Jun 2011

$$T_S = T_{RF} = \frac{-\phi(v_C)}{2\pi v_{RF}} \tag{3}$$

where the phase shift at the center of SBS ($\varphi(v_C + v_{RF})$) is zero. In addition, the tuning of the OC phase $\varphi(v_C)$ can be performed modulus 2π, thus a 360° OC phase-tuning is enough to perform TTD operation [19].

3. True-time delay line

The SCT technique consists of two parts: the separately tuning of the OC phase and imparting a constant group delay over the frequency range of interest Δv_{RF}. In fact, the separately tuning of the OC phase needs a frequency independent RF phase shifter. In our scheme, this is realized by a commercial *x*-cut integrated DPMZM (Photline MXIQ-LN-40) as shown in Fig. 2. The DPMZM is structured as two MZMs (MZM1 and MZM2) set in parallel and forming a third MZM (MZM3).

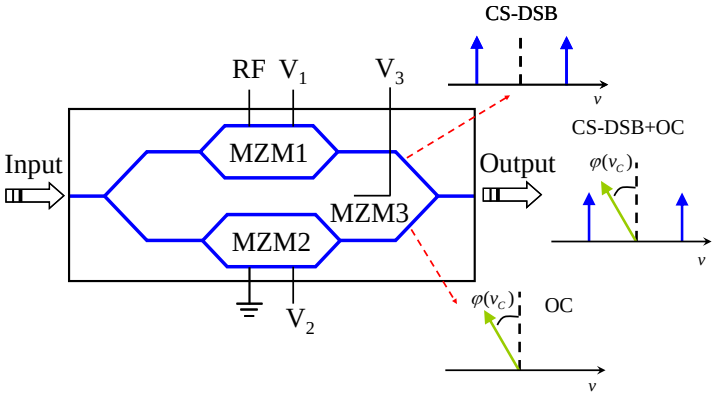

Fig. 2. Structure of the DPMZM, along with the schematic optical spectra at different locations.

In the DPMZM, MZM1 was fed by an RF signal and was biased at null point (V_1 = 7.07 V) to implement carrier suppressed-double sideband (CS-DSB) modulation. MZM2 had no driven signal and was biased at maximum transmission point (V_2 = –5.62 V) to allow the OC to pass through. They were combined together in MZM3 to achieve a CS-DSB + OC signal. A phase difference $\varphi(v_C)$ between CS-DSB and OC signals was then generated by controlling the dc bias of MZM3, V_3 [22]. When V_3 = 9.85 V, the phase difference $\varphi(v_C)$ = 0. This biased voltage of V_3 was obtained by observing the maximum output power of the DPMZM or the maximum peak of the beat note between OC and sidebands on the electrical spectrum analyzer (ESA) through a photodetector (PD). Therefore, we can independently tune the phase of OC in such modulation process. Notice, however, that the output of the DPMZM is a DSB modulated signal, which must be further processed to achieve SSB modulation.

Figure 3 depicts the schematic configuration of the TTD system. It consists of two main building blocks to realized TTD operation. The upper part performs the OC phase tuning and SBS process while the lower part of the diagram is dedicated to prepare and deliver the pump required for the implementation of SBS-based tunable delay and realize SSB modulation. The OC from a tunable laser source (TLS) emitting at 1549.952 nm was divided into two branches by an optical coupler (C1). In the upper branch, 90% OC was launched to the DPMZM, driven by the RF signal to be delayed and biased as described above, to generate a CS-DSB + OC modulated signal. An optical isolator was added to ensure unidirectional transmission.

#145830 - $15.00 USD Received 14 Apr 2011; revised 1 Jun 2011; accepted 2 Jun 2011; published 9 Jun 2011

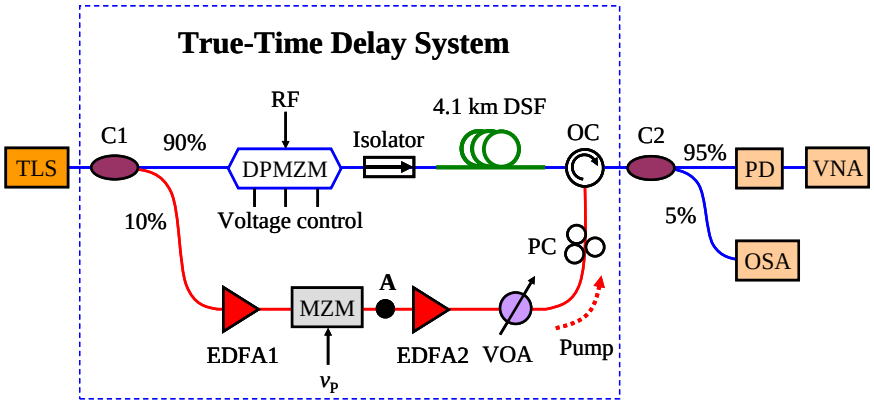

Fig. 3. Schematic configuration of the TTD system (TLS: tunable laser source; C1 and C2: optical coupler; DPMZM: dual-parallel Mach-Zehnder modulator; DSF: dispersion shifted fiber; OC: optical circulator; EDFA1 and EDFA2: erbium-doped fiber amplifier; VOA: variable optical attenuator; PC: polarization controller; PD: photodetector; VNA: vector network analyzer; OSA: optical spectrum analyzer).

In the lower branch, 10% OC was amplified by an erbium-doped fiber amplifier (EDFA1) and fed to a MZM driven by an RF signal of frequency ν_P and biased at null point to generate a CS-DSB modulated signal. This signal was then amplified by EDFA2 and acted as the pump signal. The pump power was controlled using a variable optical attenuator (VOA) to precisely adjust the amount of group delay. A polarization controller (PC) was added to control the polarization state of the pump signal in order to maximize the Brillouin interaction.

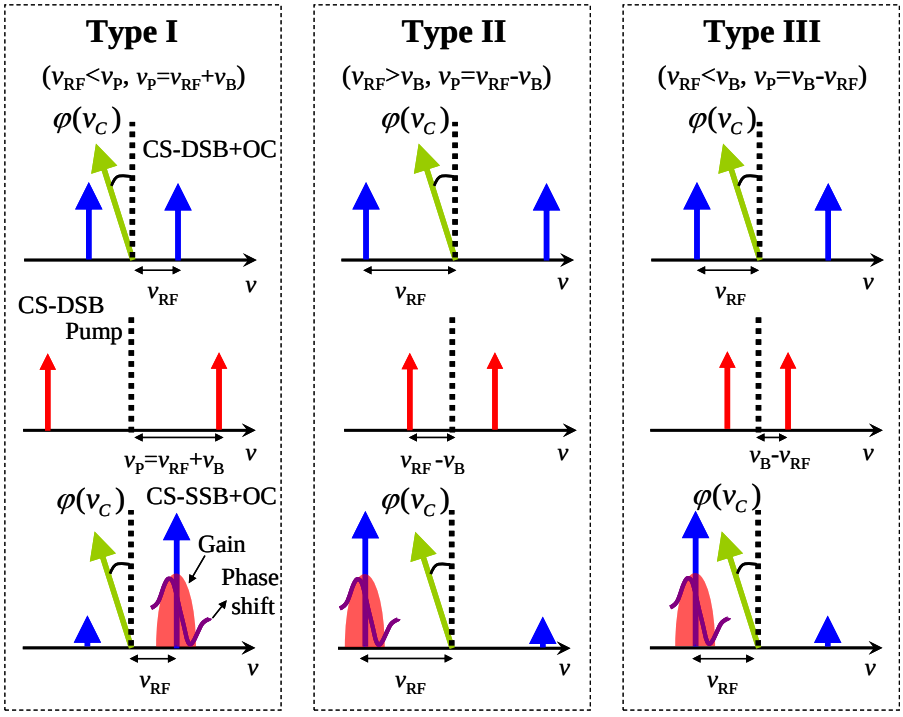

Fig. 4. Three types of CS-SSB + OC modulation are realized by counterpropagating a CS-DSB + OC signal at a frequency of ν_{RF} and a CS-DSB pump signal at a frequency of ν_P in a length of DSF: Type I ($\nu_{RF}<\nu_P$, $\nu_P = \nu_{RF} + \nu_B$), Type II ($\nu_{RF}>\nu_B$, $\nu_P = \nu_{RF}-\nu_B$) and Type III ($\nu_{RF}<\nu_B$, $\nu_P = \nu_B-\nu_{RF}$).

#145830 - $15.00 USD Received 14 Apr 2011; revised 1 Jun 2011; accepted 2 Jun 2011; published 9 Jun 2011

An optical circulator (OC) was used to counterpropagate the pump and the CS-DSB + OC modulated signals in a 4.1 km dispersion shifted fiber (DSF). DSF instead of a standard single mode fiber is employed to reduce the chromatic dispersion introduced in the TTD line. In the DSF, SBS generates both Brillouin gain and loss. The central frequencies of the Brillouin gain and loss profiles are down-shifted and up-shifted by ν_B (the Brillouin frequency) from the pump frequency, respectively. For the 1549.952 nm pump signal, the Brillouin frequency ν_B was measured to be 10.492 GHz for the DSF used in the experiment. By properly setting the driven frequency ν_P of the MZM in the lower branch, we can achieve that one sideband of the CS-DSB + OC modulated signal locating at the Brillouin loss profile suffers attenuation, while the other sideband of the Stokes signal locating at the Brillouin gain profile is consequently amplified [23]. Therefore, CS-SSB + OC modulation and SBS-induced slow light (within the Brillouin gain profile) were simultaneously achieved. Figure 4 shows three types of SBS-induced slow light and CS-SSB + OC modulation configuration: Type I ($\nu_{RF}<\nu_P$, $\nu_P = \nu_{RF} + \nu_B$), Type II ($\nu_{RF}>\nu_B$, $\nu_P = \nu_{RF}-\nu_B$) and Type III ($\nu_{RF}<\nu_B$, $\nu_P = \nu_B-\nu_{RF}$). The Brillouin gain and SBS-induced optical phase shifting spectra are also illustrated in Fig. 4.

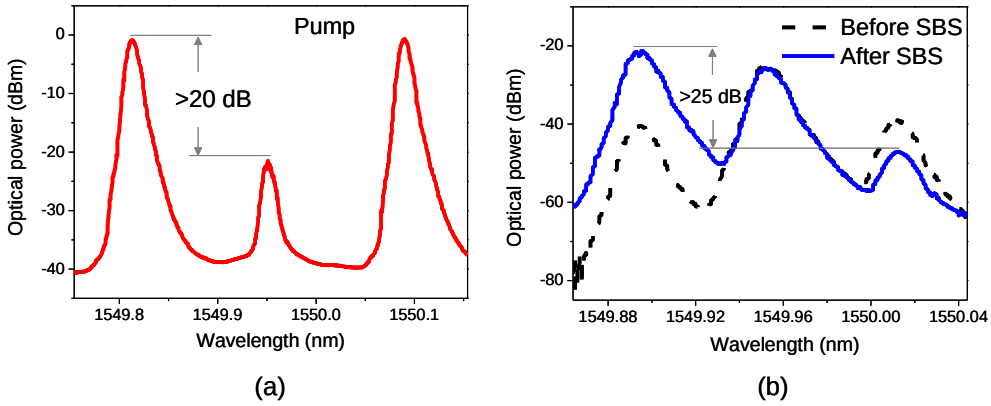

Fig. 5. Measured optical spectra of the (a) pump, (b) CS-DSB + OC modulated (before SBS), and CS-SSB + OC modulated (after SBS) signals for Type I modulation (ν_{RF} = 8 GHz, ν_P = 18.492 GHz).

Figure 5 shows the measured optical spectra of the pump, CS-DSB + OC modulated (before SBS), and CS-SSB + OC modulated (after SBS) signals for Type I modulation. The RF signal from a vector network analyzer (VNA) at the frequency of 8 GHz (ν_{RF}) with RF power of 13 dBm was fed to the DPMZM. To implement the Type I modulation, the MZM driven frequency ν_P was set at 18.492 GHz with RF power of 2 dBm. The optical spectrum of the pump signal, as shown in Fig. 5(a), was measured at point A (see Fig. 3). The residual OC is show to be 20 dB below the sidebands. This suppression ratio was sufficient to avoid having the residual OC induce any significant Brillouin gain or loss. The pump power injected into the DSF was 12.7 dBm. Figure 5(b), measured from the 5% port of C2 (see Fig. 3), shows the optical spectra of the CS-DSB + OC modulated (before SBS) and CS-SSB + OC modulated (after SBS) signals, where the upper-frequency sideband of the CS-DSB + OC modulated signal is amplified by the upper-frequency sideband of the pump signal, while the lower-frequency sideband of the CS-DSB + OC modulated signal is consequently attenuated by the lower-frequency sideband of the pump wave in the SBS process. The CS-SSB + OC modulation has an undesired sideband suppression ratio (USSR, i.e. the power ratio of the amplified sideband and the attenuated sideband) of larger than 25 dB as shown in Fig. 5(b).

Figure 6 shows the measured USSR versus ν_{RF} for a fixed pump power of 14.4 dBm. More than 27 dB of USSR was achieved from 4 to 20 GHz for different types of CS-SSB + OC modulation configuration. The variations in the USSR were mainly attributed to the frequency response of the DPMZM. For ν_{RF} = 10.492 GHz, the MZM in the lower branch of the TTD system was saved since the pump signal was provided by the OC. The measurement from 4 to

#145830 - $15.00 USD Received 14 Apr 2011; revised 1 Jun 2011; accepted 2 Jun 2011; published 9 Jun 2011

20 GHz was limited by the 0.01nm resolution bandwidth of optical spectrum analyzer (OSA) and the bandwidth of the devices employed. In principle, arbitrarily high RF signal with CS-SSB + OC modulation could be performed if high-frequency devices could be available.

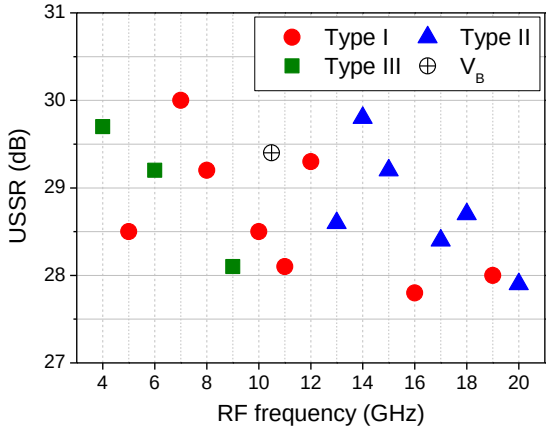

Fig. 6. Measured USSR versus v_{RF} for a fixed pump power of 14.4 dBm. Different types of CS-SSB + OC modulation configuration were used in the measurement.

When the CS-SSB + OC modulated signal (see Fig. 5(b)) was detected by the PD, the phase shift of the OC is directly translated to the conveyed RF signal. Note that the RF phase shift is independent of the RF frequency. Figure 7 shows a nearly linear phase shift of the 8 GHz RF signal with respect to the bias voltage (V_3) of the DPMZM. The VNA was calibrated under V_3 = 1.27 V. A full 360° RF phase shift was achieved when the dc bias of the DPMZM was tuned from −13.3 to 15.72 V. This is essential requirement to compensate any value of $\varphi(v_C)$ for TTD operation.

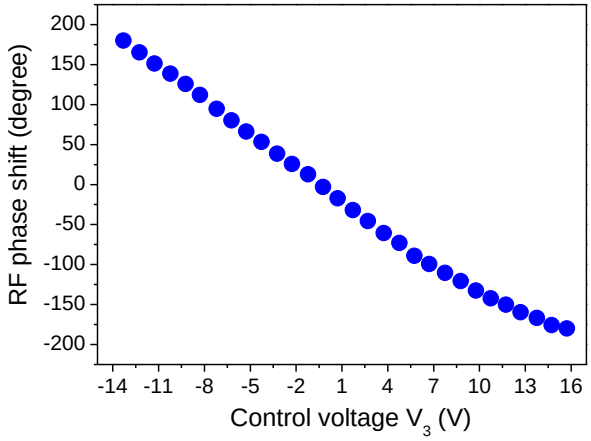

Fig. 7. Phase shift of the 8GHz RF signal with respect to the control voltage (V_3) of the DPMZM.

In our scheme, the SBS process is not only used to achieve SSB modulation, but also used to induce a linear phase shift in the vicinity of the SSB modulation sideband. Figure 8 shows the phase of the RF signal as a function of the RF frequency in the vicinity of 8 GHz while the pump power of the SBS delay line is varied. For each pump power, the RF phase shift exhibits a linear variation with respect to the RF frequency in a 15 MHz frequency range centered at 8 GHz. The time delay varies from 2.5 to 24 ns while the pump power is changed

#145830 - $15.00 USD Received 14 Apr 2011; revised 1 Jun 2011; accepted 2 Jun 2011; published 9 Jun 2011

from 5.7 to 14.4 dBm. For TTD operation, the OC phase shift has to be adjusted for each delay by tuning the dc bias of the DPMZM. Therefore, the SCT delay line can operate as a TTD element, providing a tunable TTD up to 24 ns with an instantaneous RF bandwidth of 15 MHz.

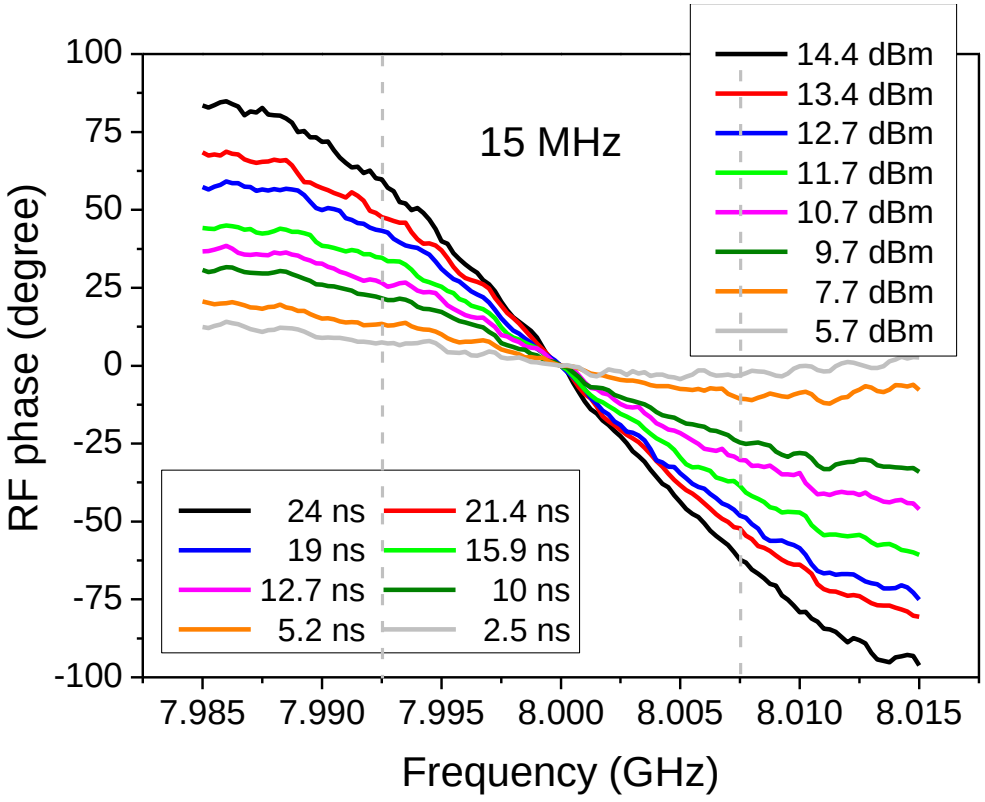

Fig. 8. The phase of the RF signal measured by the VNA as a function of the RF frequency in the vicinity of 8 GHz while the pump power of the SBS delay line is varied.

Figure 9(a) shows the spectral profile of the SBS gain resonance while the RF frequency ν_{RF} was swept in the vicinity of the resonance with pump power of 13.4 dBm. A moderate amplitude change of 3 dB is observed in a 15 MHz frequency range. The USSR of the CS-SSB + OC modulated signal (ν_{RF} = 8 GHz) with respect to the pump powers is shown in Fig. 9(b). Note that a short delay time needs a low pump power, which results in a low USSR. The low USSR will affect the SSB performance of the system. Hence there is a trade off between the high USSR and the short delay time. A possible method to overcome this problem is to broaden the SBS bandwidth by pump modulation [12–15]. Since the maximum achievable delay is inversely proportional to the SBS bandwidth, a broadened SBS bandwidth may lead to a short group delay while preserving high pump power as well as high USSR.

#145830 - $15.00 USD Received 14 Apr 2011; revised 1 Jun 2011; accepted 2 Jun 2011; published 9 Jun 2011

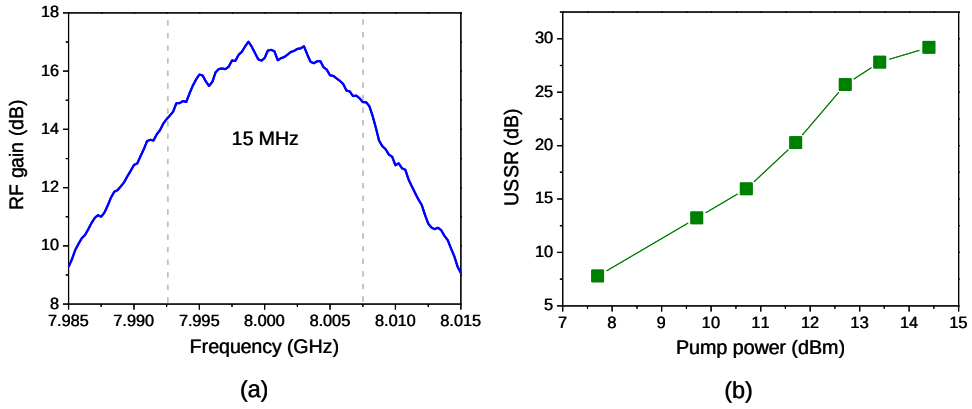

Fig. 9. (a) SBS gain profile and (b) the USSR of the CS-SSB + OC modulated signal (ν_{RF} = 8 GHz) with respect to the pump powers.

4. Reconfigurable microwave photonic filter

In order to verify the feasibility of the proposed TTD line, we applied it for a reconfigurable MPF. Figure 10 depicts the schematic configuration of a two-tap incoherent MPF. The transfer function of this structure is given by

$$H(\nu) = a_1 + a_2 \cdot e^{-i(2\pi\nu T)}. \quad (4)$$

where a_1 and a_2 are the filter taps coefficients that can be real or complex, and T is the basic delay of the filter.

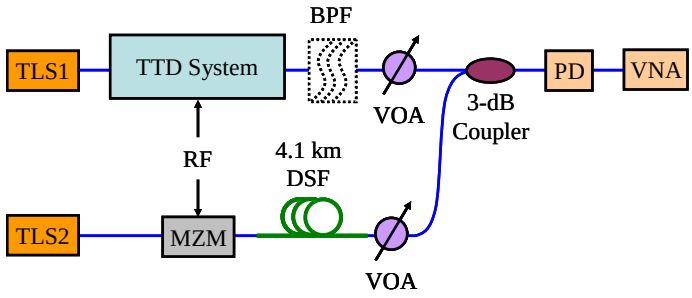

Fig. 10. Schematic configuration of a two-tap incoherent MPF. TLS1 and TLS2: tunable laser source, TTD system: true time delay system (as illustrated in Fig. 3), BPF: tunable optical band-pass filter, MZM: Mach-Zehnder modulator; DSF: dispersion shifted fiber; VOA: variable optical attenuator, PD: photodetector, VNA: vector network analyzer.

Two distinct tunable laser sources (TLS1 and TLS2) were used in the experiment. They are naturally incoherent. Thus, the minimal time delay in the filter is not limited by the coherence length of the laser and it makes possible to achieve a higher free spectral range (FSR) for the filter [19]. The frequency distance between two lasers was adjusted at 100 GHz (TLS1: 1549.952nm, TLS2: 1549.152 nm) to avoid signal distortion caused by the beating signal between two lasers. The RF signal from the output port of the VNA was split by an RF power splitter. Then the two same RF signals were applied to the DPMZM and a conventional signal-driver MZM. Light outputs from TLS1 and TLS2 were fed to the DPMZM and the signal-driver MZM, respectively. The real coefficient of the filter is generated in the lower arm. The upper arm was used to implement tunable TTD operation. Two VOAs were added to provide amplitude balance between the two arms. Then the optical signals from two arms were combined to mutually interfere in the PD by a 3-dB optical coupler and the filter frequency response was measured by the VNA.

#145830 - $15.00 USD Received 14 Apr 2011; revised 1 Jun 2011; accepted 2 Jun 2011; published 9 Jun 2011

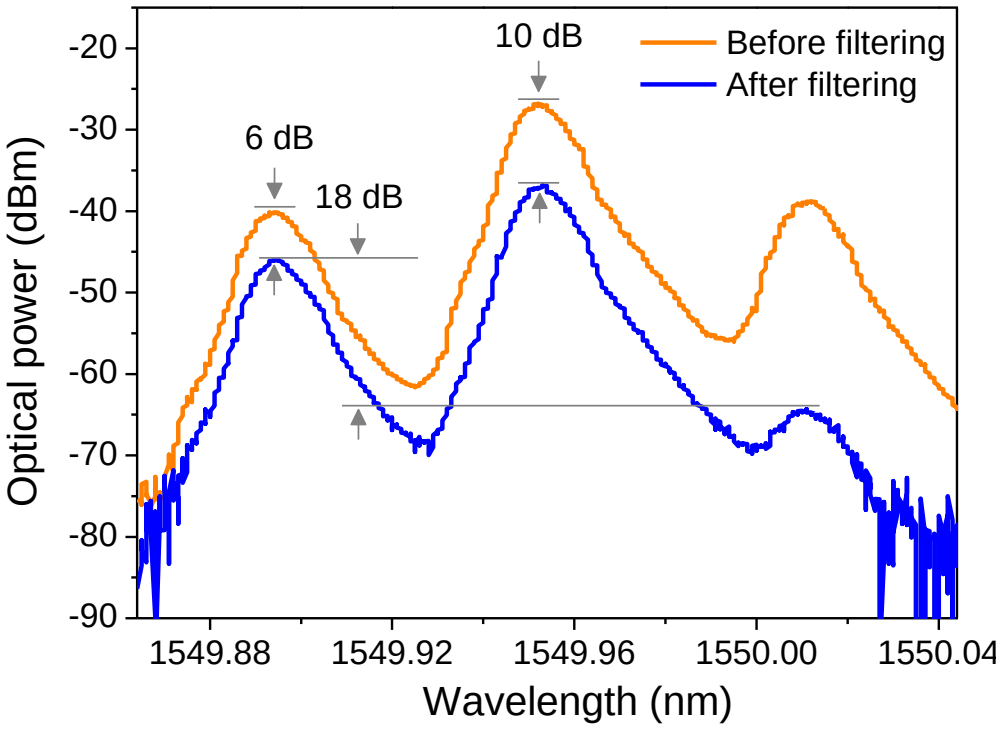

Fig. 11. Measured optical spectra before and after the BPF.

To check the filter tunability, we first measured the basic delay of the filter when pump in the TTD system was turned off. In order to realize SSB modulation without using the SBS, we added a tunable band-pass filter (BPF) after the TTD system to block the lower frequency sideband of the CS-DSB + OC modulated signal as shown in Fig. 10. The optical spectra before and after the BPF are shown in Fig. 11. The modulation frequency (ν_{RF}) was 8 GHz. USSR of 18 dB was achieved.

#145830 - $15.00 USD Received 14 Apr 2011; revised 1 Jun 2011; accepted 2 Jun 2011; published 9 Jun 2011

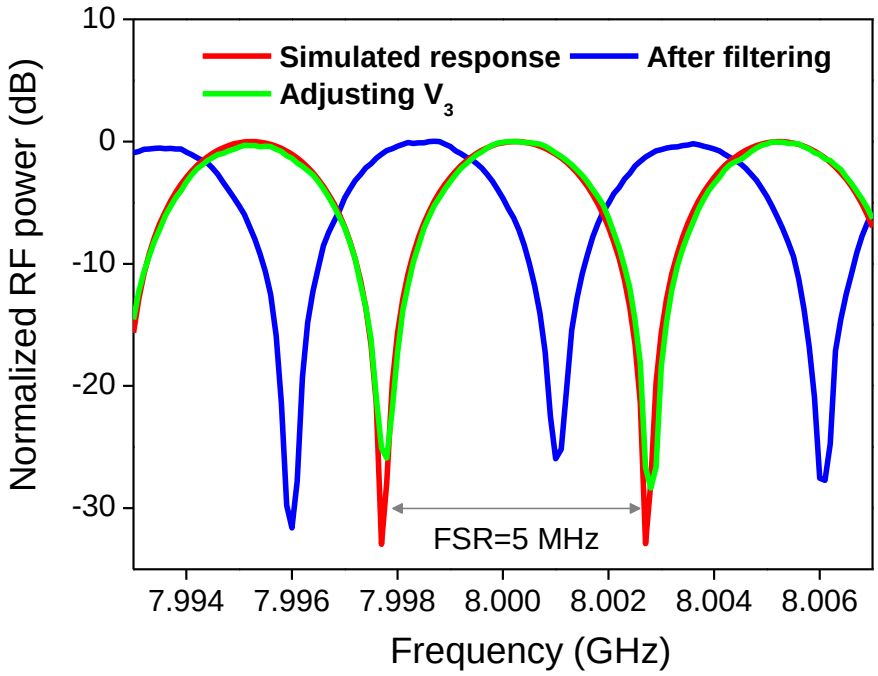

Fig. 12. Measured (blue line, after filtering and green line, by adjusting V_3) and simulated (red line) frequency response of the MPF.

Figure 12 shows the measured filter response (blue line) when the bias voltage of the DPMZM, V_3, was adjusted to 9.85 V. In this case, the phase difference $\varphi(v_C)$ between CS-DSB and OC signals at the output of DPMZM is zero. The two branches of the MPF have a path imbalance of 40 m, corresponding to T_0 = 200 ns and resulting in a FSR of 5 MHz. However, this filter response is not matched with the simulated result (red line) as shown in Fig. 12. Although their FSRs are equal, their notch positions are different. This can be explained as follows: the BPF introduced 6 and 10 dB optical power attenuations to the upper frequency sideband and the OC, respectively, as shown in Fig. 11. It means that the OC was located at the edge of the BPF bandwidth and thus suffered more attenuation than the upper frequency sideband. Therefore, the BPF will introduce a phase shift $\varphi_{BFP}(v_C)$ to the OC just as the FBG [18]. In this case, the filter response can be expressed as

$$H'(v) = a_1 + a_2 e^{i\varphi_{BPF}(v_C)} e^{-i(2\pi vT)} = H(v - \frac{\varphi_{BPF}(v_C)}{2\pi T}). \quad (5)$$

The notch positions of the filter are changed by $\varphi_{BFP}(v_C)/ 2\pi T$. However, this phase shift $\varphi_{BFP}(v_C)$ can be compensated by adjusting the dc bias of the DPMZM, V_3, which also introduces a phase shift to OC, as shown in Fig. 12 (green line). It must be pointed out that, by adjusting V_3, the notch position of the filter is varied while maintaining the shape and the FSR of the frequency response unchanged since the TTD between the two arms of the filter is fixed.

Next, we implemented a SBS-induced delay in the upper branch of the filter. In this case, the BPF was replaced by a short fiber which was used to compensate the time delay introduced by the BPF. The SCT technique predicts that a TTD can be generated, which must lead to a different FSR of the MPF since the time delay is changed [18,19]. Figure 13 confirms that the FSR of the MPF changes when the pump signal (13.4 dBm, Type I modulation) was applied. The SBS generated a time delay of ~21.4 ns with ~15 MHz bandwidth. This means that the FSR should be increased up to 5.6 MHz. In this case, for TTD

#145830 - $15.00 USD Received 14 Apr 2011; revised 1 Jun 2011; accepted 2 Jun 2011; published 9 Jun 2011

operation, −154° of OC compensation is needed, according to Eq. (3). Figure 13 shows an excellent agreement of the measured and the simulated frequency responses of the MPF without and with SBS process.

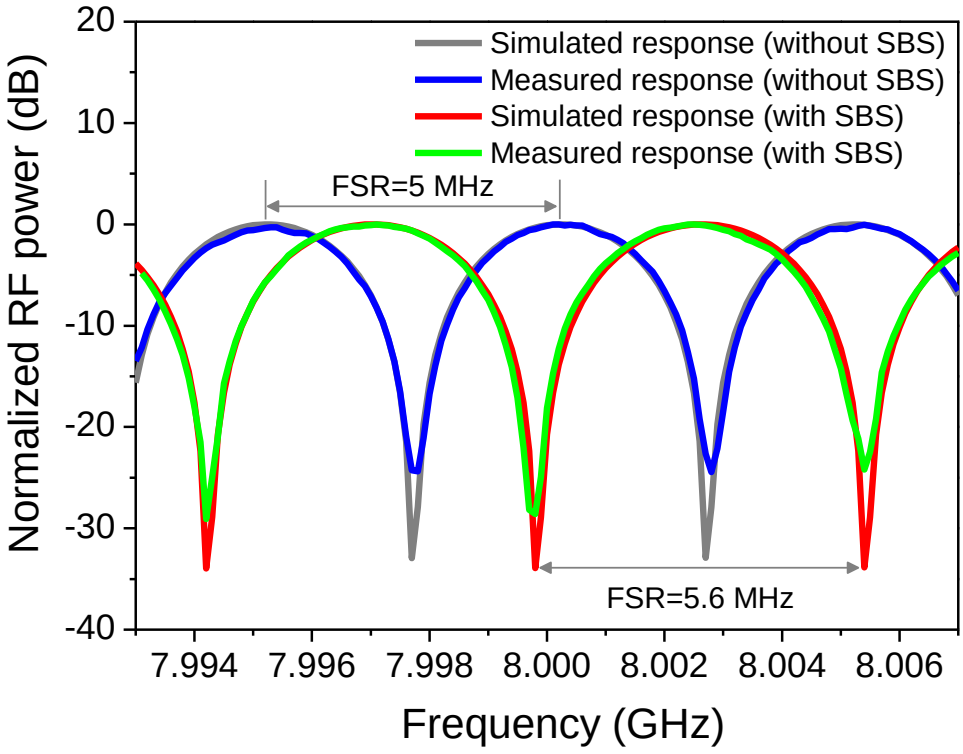

Fig. 13. Measured and simulated frequency response of the MPF without and with SBS process.

5. Conclusion

We have experimentally demonstrated a tunable TTD line with SCT using DPMZM and SBS-induced slow light. The configuration to realize TTD consists of two main blocks: photonic RF phase shifter which is independent of RF frequency and SBS-based slow light. The separate tuning of the OC phase up to 360° has been simply achieved by adjusting the bias voltage of the DPMZM. Moreover, the SBS process was not only used to introduce a constant group delay across the RF bandwidth of interest, but also used to realize SSB modulation. Three types of SBS-induced slow light and SSB modulation configuration have been demonstrated. Finally, the TTD operation of the proposed method has been clearly verified by the two-tap MPF as the FSR of the filter was varied.

It should be pointed that the center frequency of the RF signal is frequency-tunable. The RF signal of 8 GHz was arbitrarily chosen in the experiment. In principle, the proposed technique works for arbitrarily high RF, which is only limited by the bandwidth of the optical transmitter and receiver employed. The SBS-induced delay time and signal bandwidth can be controlled by using the pump modulation method [12–15]. The bandwidth of the SBS can be broadened up to its limit (~12 GHz) [24] which can allow us to operate the system at larger RF bandwidth.

#145830 - $15.00 USD Received 14 Apr 2011; revised 1 Jun 2011; accepted 2 Jun 2011; published 9 Jun 2011

Acknowledgments

This work was supported by the Meteorology Industry Research Project of China under GYHY200806033 and GYHY201006045, the National Natural Science Foundation of China under 61021003, 61090391, 60837001, and 60820106004, the National Basic Research Program of China under 2009AA03Z409, and Open Fund of Key Laboratory of Information Photonics and Optical Communications (Beijing University of Posts and Telecommunications), Ministry of Education.

#145830 - $15.00 USD Received 14 Apr 2011; revised 1 Jun 2011; accepted 2 Jun 2011; published 9 Jun 2011